K. P. Lijesh
Department of Mechanical Engineering
Indian Institute of Technology Delhi,
New Delhi 110016, India
e-mail: lijesh_mech@yahoo.co.in

Harish Hirani
Associate Professor
Department of Mechanical Engineering
Indian Institute of Technology Delhi,
New Delhi 110016, India
e-mail: hirani@mech.iitd.ac.in

Development of Analytical Equations for Design and Optimization of Axially Polarized Radial Passive Magnetic Bearing

In the present research work, analytical equations have been developed for design and optimization of radial axial polarized passive magnetic bearing (PMB) with single layer for facilitating easy and quick solution, obviating the need of costly software. Seven design variables: eccentricity, rotor width, stator width, rotor length, stator length, clearance, and mean radius were identified as the main factors affecting the design and were thus considered in the development of analytical equations. The results obtained from the developed analytical equations have been validated with the published results. The optimization of the bearing design, with minimization of magnet volume as the objective function, was carried out to demonstrate the accuracy and usefulness of the developed equations. [DOI: 10.1115/1.4028488]

Introduction

The contact-free operation, high rotational speeds, zero wear, and absence of lubricant are the major advantages of bearings made of rare-earth permanent magnets, making them an ideal contender for being maintenance-free bearing. The PMB employing rare-earth permanent magnets consists of rotor and a stator made up of magnetic rings arranged in either repulsive or attractive mode [1]. The arrangements of these magnets causes separation (levitation) of the rotor from the stator and introduces the unique advantages of contact-free operation, high rotational speeds, zero wear, and absence of lubricant, making them maintenance-free bearing [2,3].

The PMB is designed to support a given load subjected to the constraints of length, diameter, etc. Design of such bearings requires solution of complex equations, which is necessitated due to the dependence of its performance on a large number of geometric and operational parameters. The design validation of the PMB is carried out by conducting analysis using finite element method (FEM) [3,4], three-dimensional (3D) numerical methods [5,6], semi-analytical methods [7,8], and analytical methods [9–11]. Even though the FEM and 3D numerical method give accurate results as compared to the analytical or semi-analytical methods, but they involve complex formulation requiring more computational time and effort. On other hand, use of analytical equations [9–11], which are incomplete in many ways, is difficult to justify. The aim of the present research is to propose a simpler, less complex, faster, and accurate method of predicting the magnetic levitation force and stiffness by developing analytical equations.

Yonnet et al. [9] calculated the magnetic forces using analytical formulae by accounting the corrective coefficient for curvature and concluded the necessity of 3D calculations, if bearing length is either shorter compared to air gap or lesser than the magnet width. Paden et al. [11] provided analytical 2D expressions for radial and axial peak load/stiffness for a stacked structure radial magnetic bearing, assuming the mean radius of the bearing much greater than width of the magnets. In the study of Paden et al. [11], the width of the rotor and stator magnets were considered equal and axial length of the magnet was much higher than the combined length of two stacked magnets.

Yonnet et al. [10] provided an analytical expression for calculating the stiffness of the radial bearing considering radial clearance, mean radius, same width and length (n), radial clearance, and mean radius as variables. As per Yonnet et al. [10], with the increase the stiffness by factor "ln n," the volume of the magnet increases by n^2. As per Moser et al. [3] for a given outer radius of the rotor magnet, the maximum stiffness of bearings occurs at certain ratio of outer radii of rotor and stator.

Optimum design of magnetic bearing for given load and constraints requires simultaneous solution of numerical equations [7], for maximizing force and stiffness values or by estimating the maximum stiffness by number of simulation for different values of parameters using FEM [3].

The use of analytical equations for the optimum design is justified only when the accuracy of the result is comparable with that obtained by numerical methods such as FEM. Therefore, an attempt has been made to develop analytical equations for determination of magnetic levitation force and stiffness considering the: (i) eccentricity, (ii) rotor width, (iii) stator width, (iv) rotor length, (v) stator length, (vi) clearance, and (vii) mean radius that gives an accuracy matching with that arrived by using numerical methods. The analytical equations were developed for particular range of variable values and the result obtained were compared with that available in literature. The minimum and maximum values were considered for defining the range of the variables after conducting survey of literature [4,5,12–14]. Since seven variables were considered for developing the analytical equations, the order of the variables for developing the analytical equations were decided based on their relative significance determined by conducting statistical analysis. A basic equation was proposed and by analyzing the trend of the variation with respect to the variable, corrective factor was incorporated. The results obtained by employing developed analytical equations were compared with the established results [5,11–13,15]. The computational time estimated for obtaining the solutions was found to be less than 1% of the time taken in obtaining solution using the numerical methods.

The optimization of the design for minimization of magnet volume was carried out. The optimum design, when compared with the conventional designs, showed a significant reduction in

Contributed by the Tribology Division of ASME for publication in the Journal of Tribology. Manuscript received May 1, 2014; final manuscript received August 25, 2014; published online October 6, 2014. Assoc. Editor: Bugra Ertas.

Table 1 Range of variables

	Tan et al. [5]	Samanta and Hirani [15]	Muzakkir et al. [12]	Fengxiang et al. [13]	Minimum–Maximum
R_1 (m)	0.01	0.01	0.005	0.0025	
$R2$ (m)	0.019	0.016	0.024	0.0075	
R_3 (m)	0.021	0.019	0.025	0.0081	
R_4 (m)	0.03	0.026	0.05	0.0131	
L (m)	0.007	0.015	0.03	0.01	0.007–0.03
l (m)	0.007	0.015	0.032	0.01	0.007–0.032
C (m)	0.002	0.003	0.001	0.0004–0.0006	0.0004–0.003
T (m)	0.009	0.007	0.025	0.005	0.005–0.025
α	1	0.8571	0.76	1	0.76–1
R_m (m)	0.02	0.0175	0.0245	0.0078	0.0078–0.0245
b	1	1	1.066	1	1–1.066
ε	0.2–0.99	0.2–0.99	0.2–0.99	0.1–0.4	0.1–0.99

magnet volume. This also substantiated the accuracy and effectiveness of the developed analytical equations.

Identification of Design Variables

On reviewing the literature, seven variables were identified as main factors affecting force and stiffness. The ranges and levels of the identified variables were determined by surveying literature [5,12,13,15] and the same are listed in Tables 1 and 2, respectively. To understand the significance of each variable, fraction factorial table, as shown in Table 3 (each column represents factor and each row represents the level of factor), has been employed.

The relative contribution of each variable (Cont_i) on stiffness and force was estimated by computing the sum of squares [16] using Eq. (1). The force and stiffness values for particular set of variables, specified in the Table 3, were estimated using Eqs. (2) and (5), respectively,

$$\text{Cont}_i = \frac{\text{Sum of squares}_i}{\sum_{i=1}^{n} \text{Sum of squares}} \tag{1}$$

To develop curve fit equations for force and stiffness incorporating all seven identified variables, "one factor at a time" method was used. In this method, one variable is varied by keeping other variables fixed. Sequence of fitting the variables in equation was decided based on the results of Eq. (5). In other words, the first factor to be fitted needs to have the highest value of "cont" and factor fitted at the last needs to have the minimum value of "cont."

To follow the proposed methodology in the present work, a permanent magnet bearing was considered which consists of axially polarized full ring rotor magnets arranged in repulsive mode (as shown in Fig. 1). In Fig. 1(*a*), inner and outer radii of the rotor magnet are represented as R_1 and R_2, respectively. Similarly, "R_3" is the inner radius of the stator, "R_4" is the outer radius of the stator, "t" is the width of the rotor magnet ($t = R_2 - R_1$), "T" is the width of stator magnet ($R_4 - R_3$), "l" is the axial length of rotor, "L" is the axial length of stator magnets, "R_m" is the mean radius of rotor outer radius and stator inner radius $(R_3 + R_2)/2$, and "e" is eccentricity of the rotor magnet from the center of stator magnets. The direction of arrows shown in Fig. 1(*b*) indicates the direction of polarization. Literature was reviewed to decide the range of dimensions (as listed in Table 1) of the most common

Table 2 Range, factors, and levels of the variables

Factors	Range	Level 1	Level 2	Level 3	Level 4	Level 5
L (m)	0.006–0.035	0.006	0.01325	0.0205	0.02775	0.035
C (m)	0.00035–0.0035	0.00035	0.00114	0.00193	0.00271	0.0035
T (m)	0.0045–0.028	0.0045	0.01038	0.01625	0.02213	0.028
α	0.7–1.05	0.7	0.7875	0.875	0.9625	1.05
R_m (m)	0.007–0.03	0.007	0.01275	0.0185	0.02425	0.03
b	0.9–1	0.9	0.925	0.95	0.975	1
ε	0.1–0.9	0.1	0.3	0.5	0.7	0.9

Table 3 Variables values considered for sensitivity

	L	C	T	α	R_m	b	ε
	0.006	0.00035	0.0045	0.7	0.007	0.9	0.1
	0.006	0.00114	0.01038	0.7875	0.01275	0.95	0.3
	0.006	0.00193	0.01625	0.875	0.0185	1	0.5
	0.006	0.00271	0.02213	0.9625	0.02425	1.05	0.7
	0.006	0.0035	0.028	1.05	0.03	1.1	0.9
	0.01325	0.00035	0.01038	0.875	0.02425	1.1	0.1
	0.01325	0.00114	0.01625	0.9625	0.03	0.9	0.3
	0.01325	0.00193	0.02213	1.05	0.007	0.95	0.5
	0.01325	0.00271	0.028	0.7	0.01275	1	0.7
	0.01325	0.0035	0.0045	0.7875	0.0185	1.05	0.9
	0.0205	0.00035	0.01625	1.05	0.01275	1.05	0.7
	0.0205	0.00114	0.02213	0.7	0.0185	1.1	0.9
	0.0205	0.00193	0.028	0.7875	0.02425	0.9	0.1
	0.0205	0.00271	0.0045	0.875	0.03	0.95	0.3
	0.0205	0.0035	0.01038	0.9625	0.007	1	0.5
	0.02775	0.00035	0.02213	0.7875	0.03	1	0.9
	0.02775	0.00114	0.028	0.875	0.007	1.05	0.1
	0.02775	0.00193	0.0045	0.9625	0.01275	1.1	0.3
	0.02775	0.00271	0.01038	1.05	0.0185	0.9	0.5
	0.02775	0.0035	0.01625	0.7	0.02425	0.95	0.7
	0.035	0.00035	0.028	0.9625	0.0185	0.95	0.7
	0.035	0.00114	0.0045	1.05	0.02425	1	0.9
	0.035	0.00193	0.01038	0.7	0.03	1.05	0.1
	0.035	0.00271	0.01625	0.7875	0.007	1.1	0.3
	0.035	0.0035	0.02213	0.875	0.01275	0.9	0.5
Mean	0.0205	0.001926	0.016252	0.875	0.0185	1	0.5

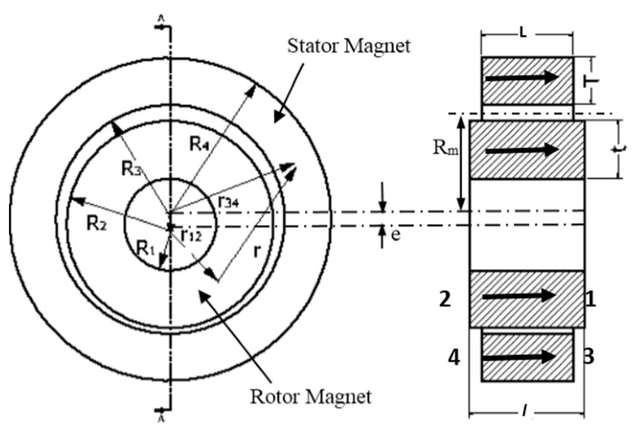

Fig. 1 Radial Magnetic bearing: (*a*) front view and (*b*) section side view

parameters. In Table 1, C $(=R_3-R_2)$ is radial clearance of the bearing, ε $(=e/C)$ is eccentricity ratio, b $(=L/l)$ is ratio of the axial lengths of the bearing, and α' is the ratio of width of the rotor to stator magnet (t/T).

The final ranges of the seven identified variables are listed in Table 2. The maximum value of eccentricity ratio (ε) is restricted to 0.9, as even slight contact in magnet asperities causes demagnetization of magnet. This value of $\varepsilon \leq 0.9$ has been decided based on the experience of authors. The magnetic surfaces are rough and the manufacturing tolerance zone of the magnet is $\pm 10\,\mu$m (value obtained from manufacturing company). Therefore, to be on safer side, $\varepsilon \leq 0.9$ was considered.

To explore the contribution of various parameters (eccentricity, rotor width, stator width, rotor length, stator length, clearance, and mean radius) toward the calculation of magnetic force and stiffness, it is necessary to conduct theoretical and/or experimental study. In the present work, theoretical study (detailed in the subsection Numerical Equations for Magnetic Bearing) has been carried out.

Numerical Equations for Magnetic Bearing. The radial forces can be calculated using the following equation [5]:

$$F_{\text{rad}} = \frac{\text{Br}_1\text{Br}_2}{4\pi\mu_0}\sum_{j=3}^{4}\sum_{i=1}^{2} f\left(\beta_{ij}\right) \tag{2}$$

where Br_1 and Br_2 are magnetic remanence of stator and rotor magnets and μ_0 is the permeability of medium between the stator and rotor; i represents face of rotor (1 or 2) and j represents face of stator (3 or 4) as shown in Fig. 1(*b*). The magnetic charges are distributed on the faces of the magnet; therefore, the total magnetic force can be calculated by the summing the forces generated by interaction between the face charges of rotor (faces 1 and 2) and stator (faces 3 and 4). In Eq. (1), $f\left(\beta_{ij}\right)$ represents the radial force and the functions can be expressed as given in Eq. (2) [5].

$$f\left(\beta_{ij}\right) = \left\{\int_0^{2\pi}\int_0^{2\pi}\int_{R_3}^{R_4}\int_{R_1}^{R_2} \frac{(e + r_{12}\cos(\theta) - r_{34}\cos(\theta'))r_{12}r_{34}}{\left(r_{12}^2 + r_{34}^2 + e^2 - 2r_{12}r_{34}\cos(\theta-\theta') + 2e(r_{12}\cos(\theta) - r_{34}\cos(\theta')) + (\beta_i)^2\right)^{1.5}} dr_{12}dr_{34}d\theta d\theta'\right\} \tag{3}$$

where β_{ij} represents the axial distance between the interacting surfaces (i.e., $\beta_{13}=0$, $\beta_{24}=L-l$, $\beta_{23}=l$, and $\beta_{14}=L$). Code for Eq. (3) was generated in MATLAB and the results were compared with the established literature [5,11–13,15].

The radial stiffness of the magnetic bearing can be found by differentiating the force equation (2) with respect to eccentricity as given in the below equation:

$$K_{\text{rad}} = \frac{dF_{\text{rad}}}{de} \tag{4}$$

The stiffness value can be calculated numerically using the central difference technique [16]. Radial force value (F_{rad}) was calculated for different eccentricity ratio (e) and radial stiffness at ith location was found using Eq. (5). The value of Δe was kept as $e/100$

$$K_{\text{rad}i} = \frac{F_{\text{rad}_{i+1}} - F_{\text{rad}_{i-1}}}{2\Delta e} \tag{5}$$

Results and Discussion. For analyzing the contribution of different factors, various levels of each factor [14] (listed in Table 3) are used. The percentage contributions of each factor for force and stiffness based on the calculated mean square [14] have been represented in Fig. 2.

From Fig. 2, it can be concluded that the contribution by four variables toward estimation of force is high (more than 11%) and three other variables contributing lesser than 9.3%. The variables α, H, and b significantly affect the stiffness value compared to the force values.

Analytical Expressions for Force and Stiffness

The analytical expression for stiffness by Yonnet et al. [10] has been given in the following equation:

$$K_{\text{r}} = \frac{\text{Br}_1\text{Br}_2}{2\mu_0}R_{\text{m}}\ln\left(\frac{(2T+C)^2C^2\left[(T+C)^2+L^2\right]^2}{(T+C)^4\left[(2T+C)^2+L^2\right](C^2+L^2)}\right) \tag{6}$$

In this expression of stiffness, T is width, L is axial length, C is clearance, and R_{m} is mean radius. Equation (6) is applicable if thickness and length of rotor are equal to those of stator. For different lengths/thickness, Eq. (6) cannot be used. In addition, the most important variable "ε" is completely missing from Eq. (6). There is need to modify Eq. (6) to incorporate all important variables. In the present work, the analytical expression has been developed which not only incorporates the variables provided in Yonnet et al. [10] equation but also incorporates the most important variable ε and other variables α and b.

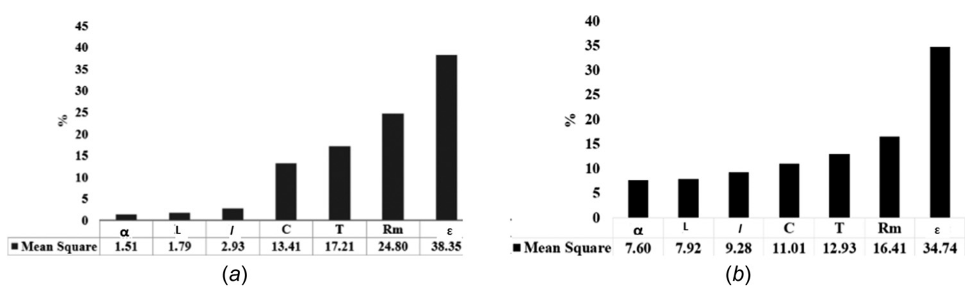

Fig. 2 Percentage mean square values: (*a*) force and (*b*) stiffness

The initial modified equations for radial force (F_r) and radial stiffness (K_r) incorporating all the seven variables have been represented in Eqs. (7) and (8) by including variables "α" (ratio of stator to rotor width), "ε" (eccentricity ratio), and "b" (ratio of rotor to stator length). Since these variables are dimensionless, they were multiplied to the variables to retain the dimension

$$F_r = \frac{Br_1 Br_2}{2\mu_0} \varepsilon C R_m \ln\left(\frac{(2T\alpha+\beta)^2 \beta^2 [(T\alpha+\beta)(T+\beta)+bL^2]^2}{\left[(T\alpha+\beta)^2 (T+\beta)^2 [(2T\alpha+\beta)(2T+\beta)+bL^2](\beta^2+bL^2)\right]} \right) \quad (7)$$

$$K_r = \frac{Br_1 Br_2}{2\mu_0} R_m \ln\left(\frac{(2T\alpha+\beta)^2 \beta^2 [(T\alpha+\beta)(T+\beta)+bL^2]^2}{(T\alpha+\beta)^2 (T+\beta)^2 [(2T\alpha+\beta)(2T+\beta)+L^2](\beta^2+bL^2)} \right) \quad (8)$$

where $\beta = C(1-\varepsilon)$. To develop the correct equations, the results obtained from Eqs. (7) and (8) were compared with the corresponding results obtained from numerical method. Subsequent to that, least square method was employed to obtain the correction coefficients to minimize the deviation in the stiffness and force values.

Determination of Corrective Coefficients. Since the eccentricity ratio "ε" is the most contributing variable, the correction coefficient for β was established first. The results were obtained from numerical equation (5) and the analytical equation (8) by varying only eccentricity value and maintaining the mean values of remaining variables (as given in Table 4) and presented in Fig. 3(*a*). It can be deduced from Fig. 3(*a*) that K_r values obtained using numerical method and Eq. (8) match at lower eccentricity ratio, but the error between the K_r values obtained from Eqs. (5) and (8) increases with increase in ε. To minimize the error, β was modified as $C(1-A\varepsilon^B)$. The value of the coefficients A and B can be estimated by using Eq. (9) for different eccentricity ratios varying from 0.1 to 0.9 with the interval of 0.02 and keeping the mean values of other variables. The number of discrete points has been increased from 5 to 41 points in order to get the best curve fit solution

$$E(x) = \frac{1}{2}\sum_{i=1}^{n}\left[\frac{F_i(x) - f_i(x)}{F_i(x)}\right] \quad (9)$$

where $E(x)$ is an error function, which is to be minimized using iterative Levenberg–Marquardt Algorithm [16], $F(x)$ is the radial stiffness value estimated from numerical equation, $f(x)$ is the radial stiffness value estimated using Eq. (8), and "n" is number of discrete points considered for curve fitting.

The values of coefficients were found as $A = 0.2$ and $B = 2$. The modified expression for C_ε is given below:

$$\beta = C\left(1 - 0.2\varepsilon^2\right) \quad (10)$$

The above procedure used for variable "ε" was repeated for the next significant variable, i.e., mean radius (R_m). Figure 4(*a*) indicates close matching in the results obtained from Eqs. (5) and (8) for R_m varying from 0.013 m to 0.03 m with interval of 0.001 m and maintaining the mean values of remaining variables. Hence, there is no need of corrective coefficient related to variable R_m. Though the range of R_m listed in Table 3 is 0.007 m to 0.03 m, *x*-axis of Fig. 4(*a*) shows variation in R_m from 0.013 m to 0.03 m. To check the validity at lower values of R_m, one example with the value of $T\alpha + C/2 < 0.007$ was considered and corresponding results are shown in Fig. 4(*b*), keeping other variables at the lowest values. This figure indicates the close matching for all values of R_m.

Similar approach was carried out for other variables. It was found that variables T, C, and L do not require any correction factor, hence no need to introduce correction coefficients corresponding to these three variables. In the case of variable α and b, correction factors are required. Figure 5(*a*) shows the comparison

Table 4 Comparison between experimental and numerical results of Tan et al. [5]

	Tan et al. [5]		
ε	Experimental (N)	Theoretical (N)	Error (%)
0.4	38	20	45.71
0.55	42	28	34.28
0.7	48	37	20.47
0.8	53	45	15.52
0.9	57	53	8.94

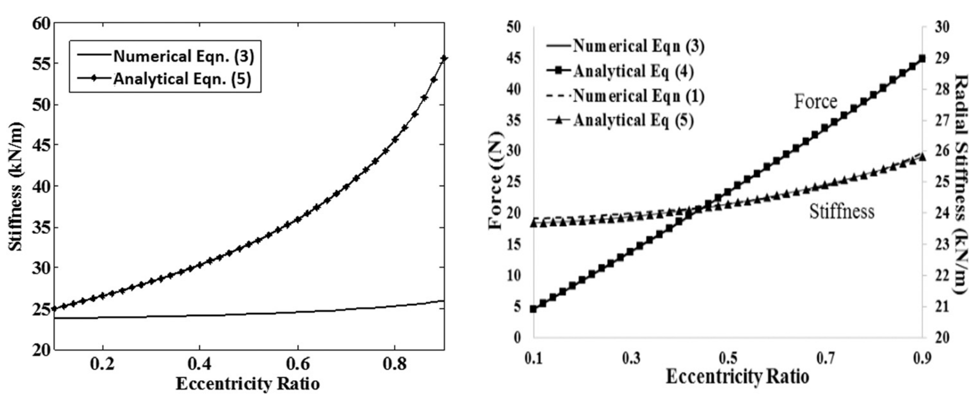

(*a*) (*b*)

Fig. 3 Comparison of numerical and analytical equations for ε: (*a*) $\beta = C(1-\varepsilon)$ and (*b*) $\beta = C(1-0.2\varepsilon^2)$

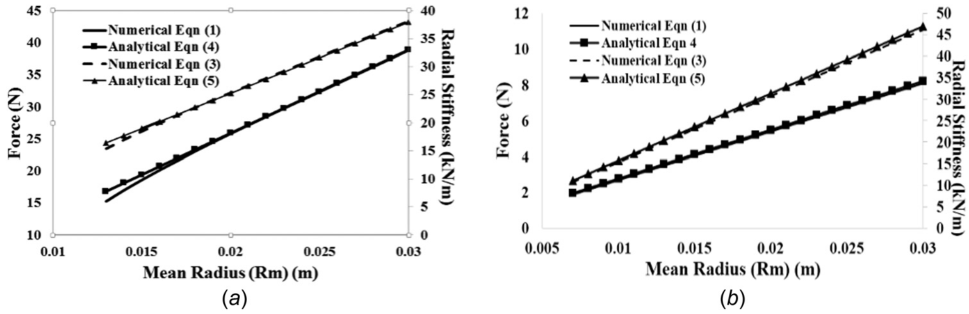

Fig. 4 Comparison of numerical and analytical methods for R_m: (*a*) mean value and (*b*) lowest value

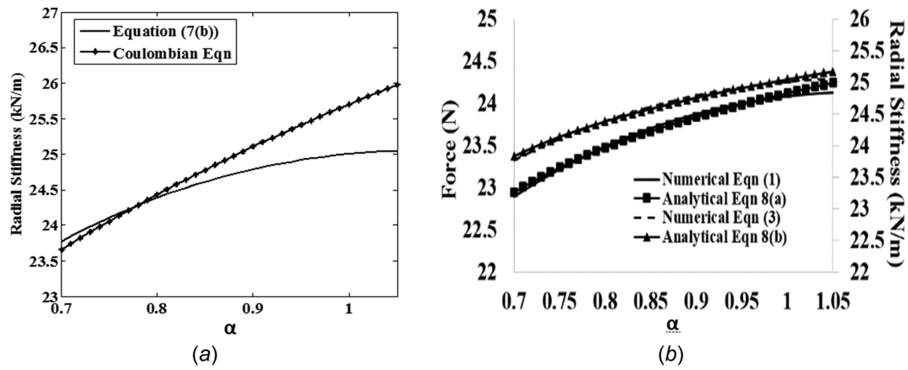

Fig. 5 Comparison of numerical and analytical equation for α: (*a*) comparison for α and (*b*) comparison for 0.9 $T'^{0.4}$ $(1-0.0111T'^{-5.4})$

in the results obtained from the numerical and analytical equations for α varying from 0.7 to 1.05 and maintaining mean values of variable C, T, L, ε, b, and R_m. From Fig. 5(*a*), it may be concluded that the values of "K_r" obtained from numerical and analytical equations match well for $\alpha = 0.7$ to 0.85, but for $\alpha > 0.85$ the values starts to diverge. The K_r curve related to numerical equation is concave downward, which indicates the need of a corrective coefficient for α. The general form of algebraic equation was defined by $Da^E(1+GT^J)$. The modified equation for force and stiffness is given in Eq. (11) and obtained values are plotted in Fig. 5(*b*).

$$F_r = \frac{Br_1Br_2}{2\mu_0}\varepsilon C R_m \ln\left(\frac{\left(1.8T\alpha^{0.4}\left(1-0.0111\alpha^{-5.4}\right)+\beta\right)^2\beta^2\left[\left(0.9T\alpha^{0.4}\left(1-0.0111\alpha^{-5.4}\right)+\beta\right)(T+\beta)+bL^2\right]^2}{\left(0.9T\alpha^{0.4}(1-0.0111\alpha^{-5.4})+\beta\right)^2(T+\beta)^2\left[(1.8T\alpha^{0.4}(1-0.0111\alpha^{-5.4})+\beta)(2T+\beta)+L^2\right]\left(\beta^2+bL^2\right)}\right) \quad (11a)$$

$$K_r = \frac{Br_1Br_2}{2\mu_0}R_m \ln\left(\frac{\left(1.8T\alpha^{0.4}\left(1-0.0111\alpha^{-5.4}\right)+\beta\right)^2\beta^2\left[\left(0.9T\alpha^{0.4}\left(1-0.0111\alpha^{-5.4}\right)+\beta\right)(T+\beta)+bL^2\right]^2}{\left(0.9T\alpha^{0.4}(1-0.0111\alpha^{-5.4})+\beta\right)^2(T+\beta)^2\left[(1.8T\alpha^{0.4}(1-0.0111\alpha^{-5.4})+\beta)(2T+\beta)+L^2\right]\left(\beta^2+bL^2\right)}\right) \quad (11b)$$

The variations in the radial stiffness using numerical and analytical equations for different values of "b" (0.9 to 1.1) have been plotted in Fig. 6(*a*). From this figure, it can be concluded that the analytical equation must be modified to account the parabolic variation in the stiffness values predicted by numerical method. The next observation is that the effect of variation of "b" is dependent on variables "C" and "L." From Fig. 6(*a*), it is observed that on decreasing clearance and increasing L, the value of stiffness increases. To account for this variation, a modified expression for b in the form of parabolic equation incorporating the variables "L" and "C" was derived. The generic parabolic equation $A_a = (1-A(b-1)^2)$ was considered so that the factor $(1-A\,(b-1)^2)$ become 1 when $b=1$. The stiffness value is maximum at $b=1$ and reduces with increase and decrease in value of "b." The final form of the equation A_a obtained from curve fit is given as $A_a = 1-2.6(L/C)^{0.7}(b-1)^2$. The modified final equation is expressed in Eq. (10). In Fig. 6(*b*), the comparison between the results obtained from the numerical and analytical equations is provided.

The final radial magnetic force analytical equation for a full ring magnet with all the correction factors is given in below equation:

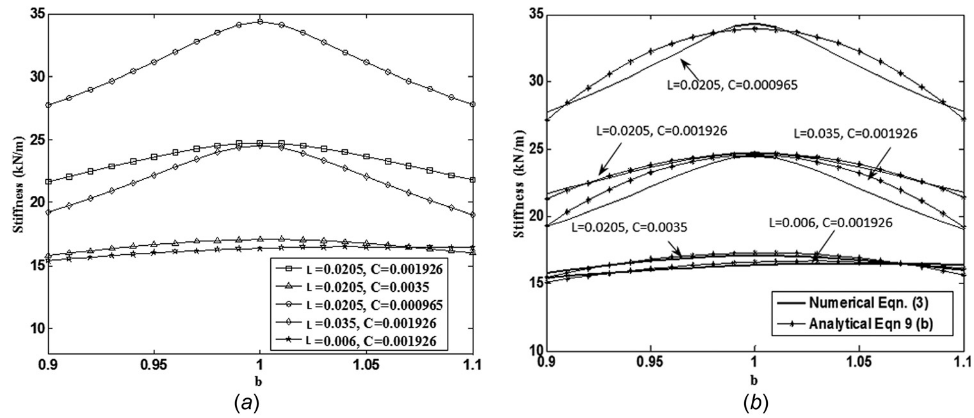

Fig. 6 Comparison of numerical and proposed equations for *b*: (*a*) Numerical equation (3) and (*b*) analytical equation (9*b*)

$$F_r = \frac{Br_1 Br_2}{2\mu_0}\left(-2.6\left(\frac{L}{C}\right)^{0.7}(b-1)^2\right)\varepsilon C R_m \times \ln\left(\frac{\left(1.8T\alpha^{0.4}\left(1-0.0111\alpha^{-5.4}\right)+\beta\right)^2\beta^2\left[\left(0.9T\alpha^{0.4}\left(1-0.0111\alpha^{-5.4}\right)+\beta\right)(T+\beta)+bL^2\right]^2}{\left(0.9T\alpha^{0.4}(1-0.0111\alpha^{-5.4})+\beta\right)(T+C_\varepsilon)\left(\beta^2+bL^2\right)\left[\left(1.8T\alpha^{0.4}(1-0.0111\alpha^{-5.4})+\beta\right)(2T+\beta)+L^2\right]}\right) \quad (12a)$$

$$K_r = \frac{Br_1 Br_2}{2\mu_0}\left(-2.6\left(\frac{L}{C}\right)^{0.7}(b-1)^2\right) R_m \times \ln\left(\frac{\left(1.8T\alpha^{0.4}\left(1-0.0111\alpha^{-5.4}\right)+\beta\right)^2\beta^2\left[\left(0.9T\alpha^{0.4}\left(1-0.0111\alpha^{-5.4}\right)+\beta\right)(T+\beta)+bL^2\right]^2}{\left(0.9T\alpha^{0.4}(1-0.0111\alpha^{-5.4})+\beta\right)(T+C_\varepsilon)\left(\beta^2+bL^2\right)\left[\left(1.8T\alpha^{0.4}(1-0.0111\alpha^{-5.4})+\beta\right)(2T+\beta)+L^2\right]}\right) \quad (12b)$$

Validation of the Proposed Analytical Equations

The developed analytical equations for force (Eq. 12*a*) and stiffness (Eq. 12*b*) must be validated against the published literatures [5,11–13,15]. The bearing dimensions considered for validation are listed in Table 1. Four cases have been considered for verifying the force expression (12*a*) and one case has been accounted to verify the stiffness expression (12*b*). To provide much more meaningful results, the dimensional eccentricity value provided in literature are represented as nondimensional eccentricity, i.e., eccentricity ratio (ε).

Case Study 1: Tan et al. [5] carried out experimental and theoretical studies on magnetic bearing for developing a hybrid hydrodynamic + magnetic bearing. Tan et al. [5] have used numerical equation to predict the load carrying capacity of the magnetic bearing. Tan et al. [5] provided experimental as well as theoretical results, as listed in Table 4. On comparing these results (third/fourth column of Table 4), considerable deviation at lower eccentricity is observed. Deviation in theoretical results from experimental observations decreases with increase in eccentricity ratio. As per Mukhopadhyay et al. [4] reason for differences in theoretical and experimental results may be due to: (i) the direct use of the coercive force values specified by the manufacturer and (ii) more possibility of error in measuring small distance compared to measuring large displacement. As in the present work, all material and geometric values have been opted from Tan et al. [5], it was decided to compare the results of proposed formulation with that of theoretical results provided by Tan et al. [5]. Table 5 provides such comparison. From this table, it can be inferred that the predicted analytical results are matching well with the numerical results by Tan et al. [5].

Case Study 2: In the second case study, Samanta and Hirani [15] estimated the theoretical load carrying capacity of the bearing to be 3.2 N for the eccentricity of 22.5 μm. The predicted value of radial force using the numerical equation (2) is 3 N and by proposed equation (12*a*) it is 3.32 N.

Case Study 3: Fengxiang et al. [13] carried out 3D FEM based analysis to find the radial load carrying capacity for three difference clearance ($C = 0.0004$ m, 0.0006 m, and 0.0008 m) with $L = 0.01$ *m*, $b = 1$, $T = 0.005$ m, $\alpha = 1$, and $R_4 = 0.0262$ mm. The eccentricity of the shaft was varied from 0 to 0.0003 m and the 3D FEM results along with the numerical equation and proposed equation have been tabulated in Table 6.

Case Study 4: Muzakkir et al. [12] carried out theoretical study using 3D numerical equation for predicting the radial load carrying capacity for the magnetic bearing. The theoretical results are tabulated in Table 7.

Case Study 5: In this case study, radial stiffness of the bearing has been compared with established literature by Yonnet et al. [10]. The dimensions of the bearing are $C = 0.001$ m, $L = T = 0.005$ m, $R_m = 0.0255$ m, $\alpha = 1$, and $Br_1 = Br_2 = 1$ T. The value of the radial stiffness estimated by Yonnet et al. [11] = 24.2 kN/m, by numerical equation (1) = 24.5 kN/m, and by proposed equation (10*b*) is 24.3.

From above five case studies, it can be concluded that the results obtained by employing the proposed analytical equations are comparable with the established results and the 3D numerical equation results.

Table 5 Comparison of Tan et al. [5], numerical, and proposed equations

ε	Tan et al. [5] theoretical (N)	Numerical Eq. (1) (N)	Proposed Eq. (10*a*) (N)
0.08	20	20.44	20.63
0.105	28	27.56	27.6
0.14	37	37.57	38.17
0.16	45	44.5	44.77
0.18	53	51.27	51.9

$Br_1 = 1.25$ T, $Br_2 = 1.25$ T, $R_m = 0.02$ m, $T = 0.09$ m, $L = 0.007$ m, $\alpha = 1$, $b = 1$, $C = 0.002$ m, and eccentricity varying from 0.008 m to 0.0018 m)

Table 6 Comparison of Fengxiang et al. [13], numerical, and proposed equations

	Fengxiang et al. [13]			Numerical Eq. (1)			Proposed Eq. (10a)		
Eccentricity (m)	0.0004 (N)	0.0006 (N)	0.0008 (N)	0.0004 (N)	0.0006 (N)	0.0008 (N)	0.0004 (N)	0.0006 (N)	0.0008 (N)
0.0001	0.9	0.8	0.8	0.92	0.93	0.98	0.92	0.9	0.95
0.0002	1.8	1.5	1.5	1.92	1.58	1.63	1.88	1.569	1.59
0.0003	2.75	2.5	2.3	2.91	2.61	2.42	2.83	2.54	2.35

Table 7 Comparison of Muzakkir et al. [12], numerical, and proposed equations

ε	Muzakkir et al. [12] (N)	Numerical Eq. (1) (N)	Proposed Eq. (10a) (N)
0.18	52	53.03	51.2
0.4	41	42.05	42.32
0.6	31	31.15	32
0.8	20	20.82	21

$R_m = 0.0245$ m, $T = 0.03$ m, $b = 1.066$, $\alpha = 0.76$, $C = 0.002$ m, $Br_1 = 0.8$ T, and $Br_2 = 1$ T

Optimization

The objective function in a magnetic bearing is either maximizing the load carrying capacity for the given volume or minimizing the volume for the given applied load. Since the proposed equation (12) is fully analytical and simple, optimizing magnetic bearing design will be relatively fast and accurate.

In the present work, optimization of three magnetic bearings, dimensions of which have been published in literature [5,12,15], have been carried out. The optimum solutions were achieved by minimizing the volume of the magnets for the given load with dimensional nonlinear multivariable constrains. The constraints considered were: shaft radius (inner radius of rotor magnet) and casing radius (outer diameter of the stator magnet) of the magnetic bearing along with the require load applied on the bearing. The bounds for the different variables were decided based on the limitation of manufacturing of magnets.

The objective function is defined by the below equation:

$$\min(\text{Vol}) = \pi\left(L\left(R_4^2 - R_3^2\right) + l\left(R_2^2 - R_1^2\right)\right) \tag{13}$$

The variable R_1, R_2, R_3, and R_4 can be defined in terms of T, t, C, and R_m as given in the below equation:

$$\left.\begin{aligned} R_1 &= R_m - {}^{C}\!/_{2} - t \\ R_2 &= R_m - {}^{C}\!/_{2} \\ R_3 &= R_m + {}^{C}\!/_{2} \\ R_4 &= R_m + {}^{C}\!/_{2} + T \end{aligned}\right\} \tag{14}$$

Based on the Eqs. (13) and (14), objective functions can be rewritten as

$$\min(\text{Vol}) = \pi(LT(T + 2R_m + C) + lt(2R_m - C - t)) \tag{15}$$

The equality constraints considering the inner radius of the rotor magnet, outer radius of the stator magnet, and the applied load are given in the below equation:

$$\begin{aligned} &R_1 - R_m + {}^{C}\!/_{2} + T\alpha = 0 \\ &R_4 - R_m - {}^{C}\!/_{2} - T = 0 \\ &F_R - \frac{Br_1 Br_2}{2\mu_0}\left(-2.6\left(\frac{L}{C}\right)^{0.7}(b-1)^2\right)\varepsilon C R_m \\ &\times \ln\left(\frac{\left(1.8T\alpha^{0.4}\left(1 - 0.0111\varepsilon^{-5.4}\right) + \beta\right)^2 \beta^2 \left[\left(0.9T\alpha^{0.4}\left(1 - 0.0111\alpha^{-5.4}\right) + \beta\right)(T + \beta) + bL^2\right]^2}{(0.9T\alpha^{0.4}(1 - 0.0111\alpha^{-5.4}) + \beta)(T + \beta)[(1.8T\alpha^{0.4}(1 - 0.0111\alpha^{-5.4}) + \beta)(2T + \beta) + L^2]\left(\beta^2 + bL^2\right)}\right) = 0 \end{aligned} \tag{16}$$

where R_{11}, R_{44}, and F_R are the given inner radius of the rotor magnet, outer radius of the stator magnet, and the applied load considered in different literatures. The lower bounds for the variables (t, T, and L) were considered as 1 mm due to the manufacturing, limitations, the lower bound for the clearance were considered to be 100 μm since the surface roughness of magnets is 50 μm. The load carrying capacity in different literatures was considered at eccentricity ratio of 0.9. The lower and upper bounds considered in the present case are given in the below equation:

$$\left.\begin{aligned} &0.001 \le t \\ &0.001 \le T \\ &0.001 \le L \\ &0.9 \le b \le 1.1 \\ &0.0001 \le C \\ &\varepsilon \le 0.9 \end{aligned}\right\} \tag{17}$$

The dimensions of the three published work [5,12,15] have been considered for the same load carrying capacity, inner radius of rotor, and outer radius of stator. In the present work, MATLAB has been used for obtaining the optimum solution. In MATLAB, the optimization has been carried out using minimization function (f_{min}) and "interior trust region" method for Eq. (15). The results obtained after optimization along with percentage reduction of volume have been tabulated in Table 8. From Table 8, following observation can be made: *Case Study 1*: Tan et al. [5], not much reduction in the volume is observed. It appears that they selected near optimum dimensions. This can be explained by plotting the force as a function of axial length (Fig. 7). From Fig. 7, it can be inferred that force increases with increase in length up to axial length = 0.008 m and thereafter increase is negligible. Selection of axial length equal to 0.007 m by Tan et al. [5] was a good choice. *Case Study 2*: similarly in the case of Muzakkir et al. [12], force as a function of L has been plotted in Fig. 8. From this figure, it

Table 8 Comparison of volume

	Case Study 1		Case Study 2		Case Study 3	
Parameters	Tan et al. [5]	Proposed dimension	Muzakkir et al. [12]	Proposed dimension	Samanta and Hirani [15]	Proposed dimension
C (m)	0.002	0.0026	0.001	0.0022	0.003	0.003
t (m)	0.009	0.0094	0.019	0.0130	0.007	0.0072
T (m)	0.009	0.0080	0.025	0.0298	0.006	0.0058
R_m (m)	0.02	0.0193	0.0245	0.0191	0.0175	0.0173
L (m)	0.007	0.0065	0.03	0.0172	0.015	0.006
b	1	1	1.067	1	1	1
α	1	0.85	0.76	0.43	1.1667	1.24
Force (N)	51	51	48	48	3.2	3.2
Volume (m^3)	1.583×10^{-5}	1.417×10^{-5}	2.32×10^{-4}	1.292×10^{-4}	2.219×10^{-5}	8.752×10^{-6}
% Reduction in Volume		10.5		44.3		60.6

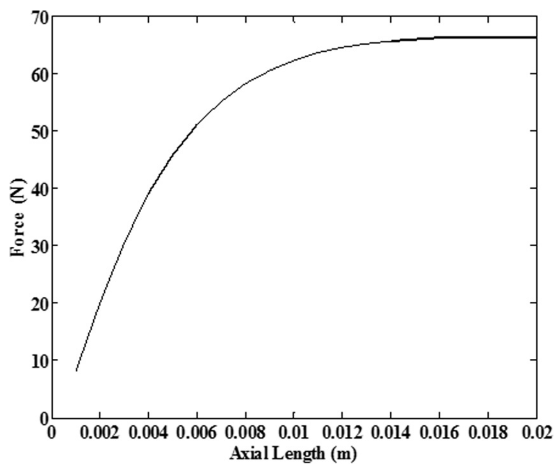

Fig. 7 Force versus L for dimensions provided in Ref. [5]

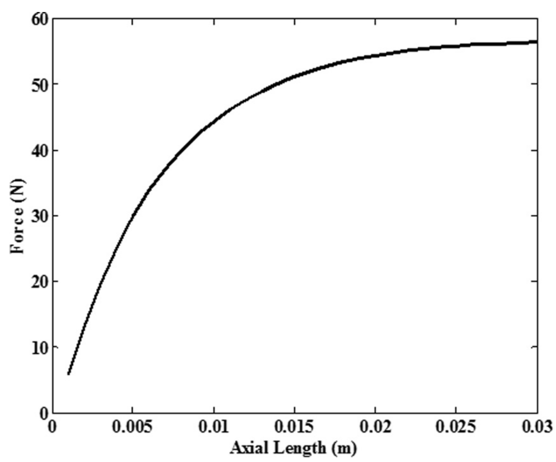

Fig. 8 Force versus L for dimensions provided in Ref. [12]

can be inferred that the increase in force is negligible for $L > 0.015$ m, but the value of L selected by Muzakkir et al. [12] was 0.03 m, hence large reduction in the volume is observed. *Case Study 3*: In the case of Samanta and Hirani [15], optimum value of L is found to be 0.006 m (Fig. 9) but they used $L = 0.015$ m. In this case also, larger reduction in volume was noticed. Note that this optimization was carried out by constraining the inner radius of rotor and outer radius of stator. The results may change if the constrains are changed and different results may be obtained. Hence, it can be concluded that using the optimization technique a better solution with a reduced volume was obtained.

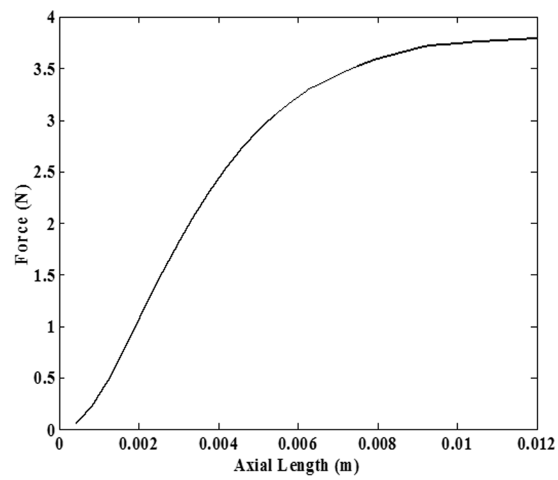

Fig. 9 Force versus L for bearing described in Ref. [15]

Conclusion

Analytical equations for the determination of magnetic force and radial stiffness of PMB with a single layer of magnets have been developed. The analytical equations include seven variables (eccentricity, rotor width, stator width, rotor length, stator length, clearance, and mean radius) which are commonly used for defining a magnetic bearing. Systematic procedures for finding contribution by each variables and curve fit method were adopted to obtain the analytical expressions. The developed analytical equations were validated against the numerical methods described in literature. Due to analytical nature of the developed equations, magnetic bearing can easily be optimized. Three magnetic bearings were optimized and appreciable saving of magnet volume was indicated. It can be concluded that with the use of the proposed analytical equations magnetic radial bearings can easily be designed with much lesser efforts. In other words, the developed analytical equations will be an aid to designers.

Acknowledgment

This research was supported by Council of Scientific and Industrial Research, New Delhi, India, Grant No. 70(0073)/2013/EMR-II.

References

[1] Yonnet, J. P., 1981, "Permanent Magnet Bearings and Couplings," IEEE Trans. Magn., **15**(1), pp. 1169–1173.
[2] Fang, J., Le, Y., Sun, J., and Wang, K., 2012, "Analysis and Design of Passive Magnetic Bearing and Damping System for High-Speed Compressor," IEEE Trans. Magn., **48**(9), pp. 2528–2537.

[3] Moser, R., Sandtner, J., and Bleuler, H., 2006, "Optimization of Repulsive Passive Magnetic Bearings," IEEE Trans. Magn., **42**(8), pp. 2038–2042.
[4] Mukhopadhyay, S. C., Ohji, T., Iwahara, M., and Member, A., 2000, "Modeling and Control of a New Horizontal-Shaft Hybrid-Type Magnetic Bearing," IEEE Trans. Ind. Electron., **47**(1), pp. 100–108.
[5] Tan, Q., Li, W., and Liu, B., 2002, "Investigations on a Permanent Magnetic–Hydrodynamic Hybrid Journal Bearing," Tribol. Int., **35**(7), pp. 443–448.
[6] Akoun, G., and Yonnet, J. P., 1984, "3D Analytical Calculation of the Forces Exerted Between Two Cuboidal Magnets," IEEE Trans. Magn., **20**(5), pp. 1962–1964.
[7] Samanta, P., and Hirani, H., 2007, "A Simplified Optimization Approach for Permanent Magnetic Journal Bearing," Indian J. Tribol., **2**(2), pp. 23–34.
[8] Ravaud, R., Lemarquand, G., and Lemarquand, V., 2009, "Force and Stiffness of Passive Magnetic Bearings Using Permanent Magnets. Part 1: Axial Magnetization," IEEE Trans. Magn., **45**(7), pp. 2996–3002.
[9] Yonnet, J. P., Hemmerlin, S., Rulliere, E., and Lemarquand, G., 1993, "Analytical Calculation of Permanent Magnet Couplings," IEEE Trans. Magn., **29**(6), pp. 2932–2934.
[10] Yonnet, J. P., Lemarquand, G., Hemmerlin, S., and Olivier-Rulliere, E., 1991, "Stacked Structures of Passive Magnetic Bearings," J. Appl. Phys., **70**(10), p. 6633.
[11] Paden, B., Groom, N., and Antaki, J. F., 2003, "Design Formulas for Permanent-Magnet Bearings," ASME J. Mech. Des., **125**(4), pp. 734–738.
[12] Muzakkir, S. M., Lijesh, K. P., and Hirani, H., 2014, "Tribological Failure Analysis of a Heavily-Loaded Slow Speed Hybrid Journal Bearing," Eng. Failure Anal., **40**, pp. 97–113.
[13] Fengxiang, W., Jiqiang, W., Zhiguo, K., and Fengge, Z., 2004, "Radial and Axial Force Calculation of BLDC Motor With Passive Magnetic Bearing," 4th International Power Electronics and Motion Control Conference, IPEMC 2004, Xi'an, China, Aug. 14–16, Vol. 1, pp. 290–293.
[14] Hirani, H., and Samanta, P., 2007, "Hybrid (hydrodynamic + permanent magnetic) Journal Bearings," Proc. Inst. Mech. Eng. Part J., **221**(8), pp. 881–891.
[15] Sung, H. P., 1996, *Robust Design and Analysis for Quality Engineering*, Chapman and Hall, London, UK, pp. 46–59.
[16] Levenberg, K., 1944, "A Method for the Solution of Certain Non-Linear Problems in Least Squares," Q. Appl. Math., **2**(2), pp. 164–168.